C.P. No. 1233

C.P. No. 1233

PROCUREMENT EXECUTIVE, MINISTRY OF DEFENCE

AERONAUTICAL RESEARCH COUNCIL

CURRENT PAPERS

The Measurement and Analysis of the Profile Drag of a Wing with a Slotted Flap

by

I. R. M. Moir, D. N. Foster and D. R. Holt

Aerodynamics Dept., R.A.E., Farnborough

LONDON: HER MAJESTY'S STATIONERY OFFICE

1972

PRICE *60 p* NET

UDC 533.6.013.122 : 533.692 : 533.694.22

* CP No.1233
August 1971

THE MEASUREMENT AND ANALYSIS OF THE PROFILE DRAG OF A WING WITH A SLOTTED FLAP

by

I. R. M. Moir**

D. N. Foster**

D. R. Holt†

SUMMARY

Measurements of lift, drag and pitching moments have been made on a wing section for a range of flap deflections, under conditions which were as close as possible to twodimensional flow. The corrected data are presented in this Report, together with the results of a semi-empirical analysis of sectional profile drag. It is shown that a consistent analysis can be made of the results over a range of flap angles and incidence, limited by a requirement for acceptable wing and flap boundary-layer conditions, precluding significant flow separations. Under these conditions, it appears that such an approach could serve as a general basis for correlating and interpreting experimental data on high-lift mechanical flap arrangements.

---

* Replaces RAE Technical Report 71158 - ARC 33663
** Aero Department, RAE, Farnborough
† Aerodynamics Design Department, Hawker Siddeley Aviation Ltd., Brough

CONTENTS

1 INTRODUCTION

The Ministry-Industry Drag Analysis Panel (MIDAP), formed in 1967 as a joint group to co-ordinate work on aircraft drag, has stated the need for an improvement in the method of estimating the drag of an aircraft with high-lift devices extended. It has suggested that, to provide a framework for the preparation of data from which improved estimates may be made, the total drag should be considered to be compounded from three components:-

$$C_D = C_{D_v} + C_{D_p} + C_{D_u} \quad (1)$$

where C_{D_v} is the linear-theory vortex drag,

C_{D_p} is the profile drag of the wing section with high-lift devices extended,

and C_{D_u} is, basically, the drag increment due to the effect of the three-dimensional nature of the flow on the boundary-layer drag, but may contain an element of the vortex drag not calculated by the linearised theory.

The last two terms may be considered as an extension, to flapped wings, of the estimation method already published[1] for the lift-dependent drag, due to the boundary layer, for plane wings.

The work of selecting and analysing the data on which estimates of the three terms in equation (1) might be based is being undertaken by Hawker Siddeley Aviation Ltd., at Brough, under Ministry of Defence (Aviation Supply) Contract No.KC/49/29/CB5D.

The characteristics of the linear theory vortex drag for a wing with part-span flaps, can be calculated directly using the computer programs based on the method of McKie[2]. As an alternative procedure, the calculated results for representative cases have been analysed and published in the form of generalised data sheets[3], related to the geometry of the wing and flap.

In view of the present lack of a quantitative method of estimating the development of the boundary layers and wakes on a wing section with high-lift devices, the data required for estimation of the boundary-layer contributions to the drag must be derived from experiments. Maskell[4] has shown that, within the same linearised assumptions as are made in the calculation of the vortex drag, it is possible to construct a theoretical framework within which to analyse measurements of the profile drag of a flapped wing section. An attempt was therefore made to correlate existing experimental measurements of the profile drag of flapped wing sections on the basis of this analysis[5]. However, it was shown that none of the considerable volume of experimental measurements examined gave consistent results when analysed in this manner. Whilst it was considered that this was, in all probability, due to the inadequacy of the experimental measurements for such purposes, it did indicate the need for a check on the validity of the analysis, using measurements made under strictly controlled conditions in a specially-designed experiment.

A series of measurements was therefore made on the RAE high-lift wing[6], under as near to twodimensional conditions as possible. Values of lift were obtained by integration of the pressure distribution measured on the model centre line, and drag was obtained by the wake survey method[7], for a range of flap deflections. As it was considered that the measured forces themselves are of intrinsic value, they have been included here, together with some brief studies of the effect of Reynolds number and transition fixing on the characteristics of the basic wing section. The experimental methods and measurements are considered in sections 2 and 3 by the RAE authors, while section 4, by the HSA author, is devoted to the analysis of these measurements.

2 EXPERIMENTAL METHODS

2.1 The model and test arrangements

The model (see Fig.1 and Table 1) was installed in the working section of the 13ft × 9ft wind tunnel at RAE Bedford for these tests and spanned the 9 ft vertical dimension of the tunnel.

In order to preserve essentially twodimensional flow conditions throughout the incidence and flap angle range, distributed suction was applied through the floor and roof adjacent to the wing junctions, via a series of holes around the fixed portion of the wing, and via perforated surfaces around the movable portions of the wing[6]. For each of the flap arrangements investigated, preliminary experiments were performed to determine the required extent of these perforations; it was found that the major part of the available perforated surfaces could be sealed by tape leaving only a narrow strip immediately adjacent to the model. The minimum suction level required to prevent flow separation at the wing/wall junctions was then determined by observation of tufts on the wing and flap; in the main experiments, slightly higher levels of suction than these minimum levels were used to ensure flow attachment at the junctions.

Tests were made on the basic model (flaps undeflected) at wind speeds of 200 ft s^{-1} and 250 ft s^{-1}, corresponding to Reynolds numbers of 3.8×10^6 and 4.8×10^6 respectively. The tests at 200 ft s^{-1} were performed both with transition free and with transition fixed at 5% chord by a 0.5 in band of 0.008 in Ballotini.

Tests were also made at 200 ft s^{-1} on the wing with a slotted flap over a range of flap deflections, the selected configurations being shown in Fig.2. An attempt was made to preserve a constant flap gap and flap/shroud overlap, but owing to limitations imposed by the design of the model, this was not fully achieved and the overlap decreased at the highest flap deflection. Transition was fixed on the upper and lower surfaces of the wing and flap at 5% chord by the same means as before.

The method of mounting the model in the tunnel precluded the direct measurement of forces and moments, and so these quantities were derived from the pressure distribution over the aerofoil. The pressure tappings were located at mid-span*; the numbers provided on each component are given in Table 2.

The pressures were digitised via eight Scanivalves and transducers, the latter having ranges of ±2.5 lb in^{-2} and ±5 lb in^{-2} (17 kN m^{-2} and 34 kN m^{-2}), the higher range being used for pressure tappings where high suctions were anticipated. The pressures were measured relative to the static pressure on the tunnel roof just upstream of the working section.

The data were reduced by a computer program which calculated the pressure coefficients and integrated them assuming a linear variation of pressure between tappings, to obtain the normal and axial force coefficients and the coefficient of pitching moment about the origin of axes, for wing and flap separately. Further manipulation of these results gave the overall lift coefficient and the coefficient of pitching moment about the quarter-chord

* Additional pressure tappings were available on the wing and flap at stations off the centre line to enable checks to be made on the degree of two-dimensionality achieved. In view of previous research[6], such checks were not considered necessary during the present experiment.

point of the basic wing. Corrections to allow for the effects of the wind tunnel walls were included in the data reduction process. Details of these are given in section 2.3.

The drag coefficient was deduced from measurements of pitot and static pressures in the wake of the model. A rake consisting of 37 pitot and 10 static tubes, the latter adjacent to every fourth pitot tube, was mounted at mid-span*, about one chord downstream of the trailing edge. Two alternative rakes were available, one with the pitots spaced 0.25 in apart and the other with 0.5 in spacing. The former was used for the tests on the basic wing,while the latter was used for tests with the flaps deflected. The rakes could be traversed normal to the airstream and rotated about the centre pitot to align them normal to the wake flow direction. The pressures in the wake were measured by transducers, but some of the pitot and static tubes were also connected to an alcohol manometer, to aid alignment of the rake. In practice, the pitot and static pressures were insensitive to misalignments of the rake of up to 10°.

The pressures on the rake were converted to coefficient form and the drag coefficient derived by the method of Jones[7].

2.2 Experimental accuracy

2.2.1 Transducers

The nominal accuracy of the transducers used during these tests is ±¼% at full-scale deflection; tests carried out at RAE have verified this. This implies that the accuracy deteriorates to about ±½% of the reading at half-scale and can be as bad as ±2% when the transducer is used over only a small portion of its range. For this reason, an attempt was made to match each transducer to the range of pressures it was expected to measure.

2.2.2 Integration of pressures

As mentioned in section 2.1, the forces on the aerofoil were obtained by integration of the pressures on the surface, assuming a linear variation of pressure between the pressure tappings. To check the accuracy of this assumption, the integration was also performed for a number of test cases by a curve-fitting method[10]; the results differed from those based on the linear assumption by less than 1%. Thus, the linear assumption is considered to be justifiable, but is dependent on close spacing of the pressure tappings in regions of high negative pressures or severe pressure gradients.

---

* Measurements of the wake drag were made only on the centre line of the model, although other sources, notably van den Berg[8], suggest that large (>30%) spanwise variations of wake drag can occur in the absence of tunnel wall boundary-layer control. However, it can be argued[9] that the application of wall suction should greatly decrease such variations.

2.2.3 Repeatability

During these tests parts of several runs were repeated. The repeatability was usually found to be better than 0.5% on C_L, with a maximum variation of 1%.

Two types of comparisons were made to test the repeatability of the drag measurements. These consisted of a direct repeat run using the same wake rake in both runs and another run using the alternative rake width. The repeated values were within 5% of the indicated profile drag coefficient.

2.2.4 Wall suction

It has been found by Foster[11], that above a certain minimum level of suction, further large increase in suction produces less than 1% change in C_L, measured at mid-span. Hence, when establishing the working suction level from observation of tufts on the model, small increases above the absolute minimum requirement should have a negligible effect on the wing characteristics measured at mid-span.

2.3 Details of corrections applied in the reduction of the data

Allowance has been made for the effect of the wind tunnel walls on the flow at the model and at the wake survey rake. These effects take the form of changes in flow velocity, relative to that obtained with an empty working section due to solid and wake blockage, together with a change in the flow direction resulting from the 'images' of the wing in the wind tunnel walls. The latter increases the effective angle of incidence of the model.

2.3.1 Solid blockage

The value of the solid blockage for the model was derived from Garner *et al.*[12] and a correction was applied to the wing and flap surface pressure coefficients only. On the assumption that the solid blockage correction for the wake survey rake and its mounting was negligibly small, no solid blockage correction was applied to the measured profile drag coefficients.

2.3.2 Wake blockage

The correction due to the wake blockage arises from the displacement effect of the model wake. For unseparated flow the correction is given by:-

$$\left(\frac{q_{corr}}{q}\right)_{uns} = 1 + \frac{1}{2} C_{D_{uns}} \frac{S}{C} \quad . \qquad (2)$$

When separation occurs on the wing ahead of the trailing edge, an additional correction is required, which according to Maskell[13] is:-

$$\left(\frac{q_{corr}}{q}\right)_s = \left(\frac{K_c}{K}\right)^2 \tag{3}$$

where

$$K^2 = 1 - C_{p_B} \tag{4}$$

and

$$K_c^2 = K^2 \left\{1 + \frac{1}{K_c^2 - 1} C_{D_s} \frac{S}{C}\right\}^{-1} . \tag{5}$$

The base pressure coefficient C_{p_B} may be easily found from the pressure distributions, but C_{D_s}, the drag increment due to flow separation could only be found approximately by estimating the pressure distribution which would have existed had the flow been attached. Because the correction resulting from the separated wake blockage is small, such an estimation of the unseparated pressure distribution is of sufficient accuracy.

The value of K_c^2 may now be found from equation (4), rewritten as a quadratic:-

$$\left(K_c^2\right)^2 - \left(1 - C'_{D_s} + K^2\right)\left(K_c^2\right) + K^2 = 0$$

where $C'_{D_s} = C_{D_s} \frac{S}{C}$, taking the root consistent with $K_c = K$ when $C'_{D_s} = 0$.

The total wake blockage correction is given by:-

$$q_{corr} = q + (\Delta q)_{uns} + (\Delta q)_s$$

therefore

$$\frac{q_{corr}}{q} = 1 + \frac{1}{2} C_{D_{uns}} \frac{S}{C} + \frac{1}{K_c^2 - 1} C_{D_s} \frac{S}{C} \tag{6}$$

and, since $C_{D_p} = C_{D_{uns}} + C_{D_s}$,

$$\frac{q_{corr}}{q} = 1 + \frac{1}{2} C_{D_p} \frac{S}{C} + \left(\frac{1}{K_c^2 - 1} - \frac{1}{2}\right) C_{D_s} \frac{S}{C} . \tag{7}$$

The correction for separated flow was only significant in the 40° flap case where it was of the order of 1% of q. The correction given by equation (7) was applied both to the lift coefficient obtained from the wing surface pressures, and to the profile drag coefficient measured by wake survey.

2.3.3 Lift constraint

Glauert[14] has shown that the effect of the images of the wing in the wind tunnel walls is to change the direction of the flow at the model by an amount $\Delta\alpha$, where

$$\Delta\alpha = \frac{\pi}{96}\left(\frac{c}{h}\right)^2\left(C_L + 4C_{m_{\frac{1}{4}}}\right) \quad . \qquad (8)$$

The values of the lift coefficient (based on basic chord) used in the determination of this correction were obtained by resolution of the normal and axial force coefficients (corrected for blockage) through the geometric angle of incidence α. The corrected angle of incidence $(\alpha + \Delta\alpha)$ was then obtained and a modified value of the lift coefficient derived by resolving the normal and axial force coefficients relative to the corrected angle of incidence.

The images of the wing in the wind tunnel walls will also result in a change of direction of the flow at the position of the wake survey rake. However, part of the experimental technique was to rotate the rake until the tubes lay in the direction of the local flow, and no associated correction to the measured results was necessary.

The lift and incidence (corrected for solid blockage, wake blockage and lift constraint effects) have been analysed subsequently in conjunction with the wake profile drag (corrected for wake blockage only).

3 EXPERIMENTAL RESULTS

3.1 Basic wing section

Figs.3, 4 and 5 give the results for lift, drag and pitching moment coefficients respectively for the basic section under the three conditions indicated on the figures. The lift curve (Fig.3) indicates that the effect of increasing the Reynolds number from 3.8×10^6 to 4.8×10^6 was to increase $C_{L_{max}}$ by about 2% and $\partial C_L/\partial\alpha$ by about 4%. Fixing transition at $R = 3.8 \times 10^6$ had negligible effect on either of these quantities.

The drag curves (Fig.4) show that the lowest drag coefficient was obtained for $R = 4.8 \times 10^6$, but that in this case and also for $R = 3.8 \times 10^6$ (transition free), a laminar 'bucket' occurred, extending from about $C_L = -0.3$ to $C_L = +0.6$. Fixing transition increased the drag coefficient throughout the incidence range but removed the 'bucket' by ensuring that the boundary layer remained turbulent from 5% chord throughout the incidence range.

The pitching-moment curves (Fig.5) are very similar for the three cases. The position of the aerodynamic centre at low incidence calculated from these curves differ very slightly, being 0.255 c_0 for both transition-free cases and 0.252 c_0 for the transition-fixed case.

3.2 Effect of flap deflection

Figs.6, 7 and 8 show the variations in lift, drag and pitching moment coefficients respectively for various flap deflections.

Table 3 summarises the values of $C_{L_{max}}$ obtained from Fig.6. It is seen that $C_{L_{max}}$ increased rapidly up to a flap deflection of 30°. Further deflection* to 40° did not result in any additional increase in $C_{L_{max}}$, because of associated separation of the flow over the flap, as shown by the pressure distribution (section 3.3).

Table 3 also gives the corresponding values of $\partial C_L/\partial\alpha$ for these curves for the range of α on which the analysis (section 4) is based. The values are given in terms of both the unextended (basic section) chord and the extended chord (which varies with flap deflection). The values of $\partial C_L/\partial\alpha$ when the flaps were deflected, based on the extended chord, are significantly higher than the value for zero flap deflection; the difference is presumably associated with differences in the nature of the boundary-layer development between the single aerofoil and the multiple aerofoil configurations, resulting from the favourable effect of the slot in the latter case. The low value at 40° deflection was again the result of flow separation from the flap.

Table 3 also gives the values of the angle of incidence at $C_{L_{max}}$. This angle decreased by approximately equal increments up to 30° flap deflection but the next 10° increment to 40° produced a much smaller change in $\alpha_{C_{L_{max}}}$.

Fig.8 shows the variation in pitching moment coefficient with C_L and Table 3 summarises the results for the positions of the aerodynamic centre at $\alpha = 0°$ derived from these curves and based on the extended chord.

---

* Note that the flap/shroud overlap was different for the 40° case; see section 2.2.

On further examination of Fig.6 it may be seen that the $C_L \sim \alpha$ curves are actually composed of two linear segments, the high-incidence segment having a smaller slope than the low-incidence segment. This is consistent with the formation of a short laminar separation bubble very close to the leading edge at the higher angles of incidence. The presence of such a bubble was confirmed by liquid film studies.

In the analysis in section 4, attention is confined to the lower segments of the lift curves to avoid conditions involving regions of significant flow separation. The restricted range of angles of incidence considered for each flap deflection is listed in Table 4.

3.3 Pressure distributions

Figs.9, 10 and 11 show the pressure distributions over the wing for three different cases: variation of incidence at zero flap deflection (basic section), variation of incidence at 30° flap deflection, and, variation of flap angle at zero incidence. Slight irregularities in the distributions, particularly near the leading-edge, are probably due to unevenness in the surface of the model. This was noticeable where the nose portion of the aerofoil joined the main part of the model.

Fig.9 shows the progressive development of the pressure distribution throughout the incidence range for the basic section. By $\alpha = 12.0^\circ$, the flow is beginning to separate at the trailing edge (this was confirmed by observation of tufting on the wing). At $\alpha = 15.5^\circ$, the flow separation is more pronounced; by this stage the wing was stalling intermittently, even with the use of the maximum level of suction available at the tunnel roof and floor, confirming that this behaviour was associated with the development of the trailing-edge flow separation. The wing stall, accompanied by a full-chord flow separation, did not occur until $\alpha = 15.73^\circ$. The stalled pressure distribution is shown as an inset to Fig.9.

The main feature of Fig.10 is the pressure distribution over the flap. This is seen to remain sensibly unchanged throughout the incidence range, an effect which is predicted by inviscid theory. A double peak in the pressure distribution is apparent at the leading edge of the flap; this arises purely from the geometry of the flap and is also predicted by inviscid theory.

Fig.11 shows the effect of flap deflection on the pressure distribution. As mentioned earlier, at 40° flap deflection the flow over the flap is seen to separate, as indicated by divergence of the pressures near the trailing edge. Incipient flow separation is also discernible at 30° deflection.

4 ANALYSIS OF LIFT/DRAG RELATIONSHIP

According to Maskell[4], linearised theoretical considerations, strictly justifiable for low C_L values only, show that the drag of a cambered aerofoil with trailing-edge flap can be represented by:-

$$\frac{C_{D_p}}{C_{D_0}} = 1 + J_1 C_L^2 + J_2 C_{L_\xi}^2 + J_3 C_{L_c}^2 + 2J_{12} C_L C_{L_\xi} + 2J_{23} C_{L_\xi} C_{L_c} + 2J_{31} C_{L_c} C_L + 0(C_L^4) \quad (9)$$

where C_{D_0} is the drag coefficient of the thickness distribution only, C_{L_ξ} and C_{L_c} are the lift coefficients due to flap angle and camber respectively, and the coefficients J_1, J_2, ... are virtually independent of the magnitude of the associated lift components.

Neglecting terms of $0(C_L^4)$, expression (9) can be reduced to:-

$$\frac{C_{D_p}}{C_{D_0}} = \frac{C_{D_m}}{C_{D_0}} + J_1\left(C_L - C_{L_m}\right)^2 \quad (10)$$

where C_{D_m} is the minimum profile drag which occurs at a lift coefficient C_{L_m}, given by:-

$$C_{L_m} = -\frac{\left(J_{12} C_{L_\xi} + J_{31} C_{L_c}\right)}{J_1} \quad (11)$$

and

$$\frac{C_{D_m}}{C_{D_0}} = 1 + \left(J_2 - \frac{J_{12}^2}{J_1}\right) C_{L_\xi}^2 + \left(J_3 - \frac{J_{31}^2}{J_1}\right) C_{L_c}^2 + 2\left(J_{23} - \frac{J_{12} J_{31}}{J_1}\right) C_{L_\xi} C_{L_c} \;. \quad (12)$$

Although this analysis is only strictly justifiable for low values of C_L and flap angle, it provides a basis whose validity can be tested for a wider range of C_L values, within a selected range of angles of incidence for each flap angle considered. Provided satisfactory empirical fits are obtainable for a variety of flapped wings, this could form a useful semi-empirical working method until a theoretical method of wider applicability has been developed.

The representation of the experimental drag by (10), (11) and (12) involved the determination of the J coefficients, but no attempt is made at this stage to interpret these values in terms of the model parameters. Essentially, the analysis involved the fitting of the experimental data to equation (10) and showing that with $J_1 C_{D_0}$ invariant with flap angle, C_{L_m} and C_{D_m} were linear and quadratic functions respectively of C_{L_ξ}. It was then necessary to show that this correlation adequately represented the experimental data over the selected ranges of incidence.

The analysis was performed for flap deflections of 10°, 20°, 30° and 40°, although examination of the $C_L \sim \alpha$ and $C_D \sim C_L$ curves, and the pressure distributions for the 40° flap deflection case indicated flow separations from the flap for all angles of incidence tested, thus it was not expected that a correlation which fitted the measured data would be obtained for this case. The basic aerofoil data were not included in view of the essential difference between this and the other configurations.

The lift due to camber, C_{L_c}, was derived from extrapolation, by the method of Least Squares, of the values of C_L at zero incidence for the flapped cases to obtain the value of C_L at zero flap angle, when $C_L = C_{L_c} = -0.052$, based on the unextended chord.

For each flap angle, equation (10) was fitted, also by the method of Least Squares, to the experimental data for various chosen values of C_{L_m}.

Results obtained from the portions of the $C_L \sim \alpha$ curves detailed in Table 4 are illustrated in Fig.12 which shows a carpet plot of C_{L_m} against $J_1 C_{D_0}$ and C_{L_ξ}. From equation (11), a linear relationship should exist between C_{L_m} and C_{L_ξ} and this is obtained for $J_1 C_{D_0} = 0.00312$, although Fig.12 shows that the relationship between C_{L_m} and C_{L_ξ} is not greatly non-linear for a wide range of values of $J_1 C_{D_0}$. Using the above value of $J_1 C_{D_0}$, the

J coefficients of equations (10),(11) and (12) were calculated and are listed in Table 5, in terms of both the basic and the extended chord.

The resulting correlation is shown in Fig.13 in which C_{D_p} is plotted against $\left(C_L - C_{L_m}\right)^2$ for all the flap angles. Fig.13 also shows the relationships obtained by inserting the calculated J coefficients in equations (10),(11) and (12) . The values of C_{L_m} given by equation (11) are listed in Table 5.

The overall correlation, in the form of C_{D_p} versus C_L, is illustrated in Fig.14, which includes points lying outside the incidence ranges specified in Table 4 and also the 40° flap deflection case.

Taking into account the inherent scatter of the experimental data, within the specified incidence ranges as indicated on the figure, the fitted curves adequately represent the measured behaviour of the wing. In particular, the values of C_{L_m}, C_D at C_{L_m} and their rates of change with incidence are accurately predicted within these limits. The average error over the selected incidence ranges is 2.1%, indicating that an acceptable correlation has been achieved.

Fig.14 also illustrates the situation outside the selected incidence ranges and also at 40° flap deflection. Both cases illustrate the profound difficulties introduced when flow separations are present.

5 CONCLUSIONS

It has proved possible to correlate measurements of lift and profile drag coefficients for a particular wing-flap combination over a limited C_L range at each of several flap angles, using a theoretical framework derived from Maskell's linearised theory. Within the ranges of angle of incidence at each flap angle for which flow separations are absent, the average error shown by the correlation is only about 2% for an overall C_L range from 0 to 2 and a flap angle range of 10° to 30°.

Table 1

DETAILS OF MODEL

Basic aerofoil section:	RAE 2815
Aerofoil chord c_0 (unextended):	3 ft (0.91 m)
Aerofoil thickness/chord ratio:	0.14
Flap chord:	0.4 c_0
Shroud trailing edge position:	0.87 c_0
Flap/shroud gap:	0.025 c_0
Flap/shroud overlap (flap leading edge to shroud trailing edge): $10^\circ \rightarrow 30^\circ$ flap deflection:	0.022 c_0
40° flap deflection:	0.006 c_0

Table 2

DISTRIBUTION OF PRESSURE PLOTTING HOLES

Component	No. of pressure tappings
Basic wing (no flap)	71
Main wing (with flap)	61
Flap	34

Table 3

SUMMARY OF RESULTS

ξ°	$C_{L_{max}}$	$\alpha^\circ_{C_{L_{max}}}$	$\frac{\partial C_L}{\partial \alpha}$ (1)	$\frac{\partial C_L}{\partial \alpha}$ (2)	$\frac{x_{ac}}{c}$ (1)
0	1.49	15.7	6.194	6.194	0.252
10	2.46	13.5	6.588	8.136	0.264
20	2.88	11.4	6.746	8.365	0.256
30	3.155	8.6	6.666	8.279	0.234
40	3.155	7.1	5.831	7.248	0.224

(1) ≡ Based on extended chord

(2) ≡ Based on unextended chord

$\frac{\partial C_L}{\partial \alpha}$ is given per radian

Table 4

RANGES OF INCIDENCE SELECTED FOR ANALYSIS

ξ^o	$C_{L_{\alpha=0}}$	Incidence range
10	0.669	$-6^o < \alpha < +7^o$
20	1.453	$-8^o < \alpha < +5^o$
30	2.190	$-10^o < \alpha < -2^o$

Table 5

VALUES OF J COEFFICIENTS AND C_{L_m}

ξ^o	C_{L_m}	$J_1C_{D_0}$	$J_2C_{D_0}$	$J_3C_{D_0}$	$J_{12}C_{D_0}$	$J_{23}C_{D_0}$	$J_{31}C_{D_0}$	
0	0.044	0.00312	0.00358	$6.872-365.6\ C_{D_0}$	-0.00134	0.055	0.00263	(1)
10	0.355	0.00385	0.00442	$8.487-451.5\ C_{D_0}$	-0.00165	0.0679	0.00322	(2)
20	0.693	0.00387	0.00444	$8.521-453.3\ C_{D_0}$	-0.00166	0.0682	0.00326	(2)
30	1.010	0.00388	0.00445	$8.535-454.1\ C_{D_0}$	-0.00166	0.0683	0.00327	(2)

(1) ≡ based on unextended chord

(2) ≡ based on extended chord

SYMBOLS

a_1	lift slope = $\partial C_L/\partial\alpha$
a_2	$\partial C_L/\partial\xi$
c_0	unextended wing chord
c	extended wing chord
C	cross-sectional area of wind tunnel
C_{D_0}	drag coefficient of thickness distribution
C_{D_v}	linear theory vortex drag
C_{D_u}	drag increment due to effect of threedimensional nature of flow on boundary-layer drag
C_{D_p}	profile drag
C_{D_s}	drag increment associated with separated flow
$C_{D_{uns}}$	drag coefficient for attached flow
C_{L_c}	lift coefficient increment due to camber
C_{L_α}	lift coefficient due to incidence
C_{L_ξ}	lift coefficient increment due to flap angle
C_{L_m}	lift coefficient corresponding to minimum drag
C_L	total lift coefficient
$C_{m_{\frac{1}{4}}}$	pitching moment coefficient about quarter-chord point
C_{p_B}	base pressure coefficient
h	width of wind tunnel
J_1, J_2, J_3, J_{12}, J_{23}, J_{31}	constants in equation for profile drag
M	Mach number
m_1	$\partial C_m/\partial\alpha$
q	measured dynamic pressure
q_{corr}	corrected dynamic pressure
Δq_{uns}	correction to q for attached flow
Δq	correction to q for separated flow

SYMBOLS (concluded)

S	reference area of model
x_{ac}	distance from leading edge to aerodynamic centre
α	angle of incidence
$\Delta\alpha$	correction to angle of incidence due to wind tunnel walls
β	$(1 - M^2)^{\frac{1}{2}}$
ξ	angle of flap deflection

REFERENCES

No.	Author	Title, etc.
1	-	Royal Aeronautical Society Data Sheets. Wings 66032 (1966)
2	J. McKie	The estimation of the loading on swept wings with extending chord flaps at subsonic speeds. ARC CP1110 (1969)
3	D.E. Rutt	Analysis of the linear theory vortex drag of plane, swept wings, with part-span non-extending chord flaps in incompressible flow. HSA (Brough) Ltd. Note YAD 3096 (1970)
4	E.C. Maskell D.A. Kirby J.Y.G. Evans	Aerodynamic research to improve the low-speed performance of transport aircraft for short or medium ranges. RAE (unpublished)
5	D.R. Holt	A report on the correlation of the profile drag of flapped wings using existing experimental data. HSA (Brough) Ltd. Note YAD 3078 (1969)
6	D.N. Foster H.P.A.H. Irwin B.R. Williams	The twodimensional flow around a slotted flap. ARC R & M 3681 (1970)
7	B. Melvill Jones	Measurement of profile drag by the pitot-traverse method. R & M 1688 (1936)
8	B. van den Berg	Some notes on twodimensional high-lift tests in wind tunnels. NLR MP 70008U (1970)
9	B. van den Berg	Unpublished communication
10	J. McKie	Unpublished communication

REFERENCES (concluded)

No.	Author(s)	Title, etc.
11	D.N. Foster J.A. Lawford	Experimental attempts to obtain uniform loading over twodimensional high-lift wings. RAE Technical Report 68283 (ARC 31098) (1968)
12	H.C. Garner E.W.E. Rogers W.E.A. Acum E.C. Maskell	Subsonic wind tunnel wall corrections. AGARDograph 109 (1966)
13	E.C. Maskell	A theory of the blockage effects on bluff bodies and stalled wings in a closed wind tunnel. ARC R & M 3400 (1963)
14	H. Glauert	Wind tunnel interference on wings, bodies and airscrews. ARC R & M 1566 (1933)

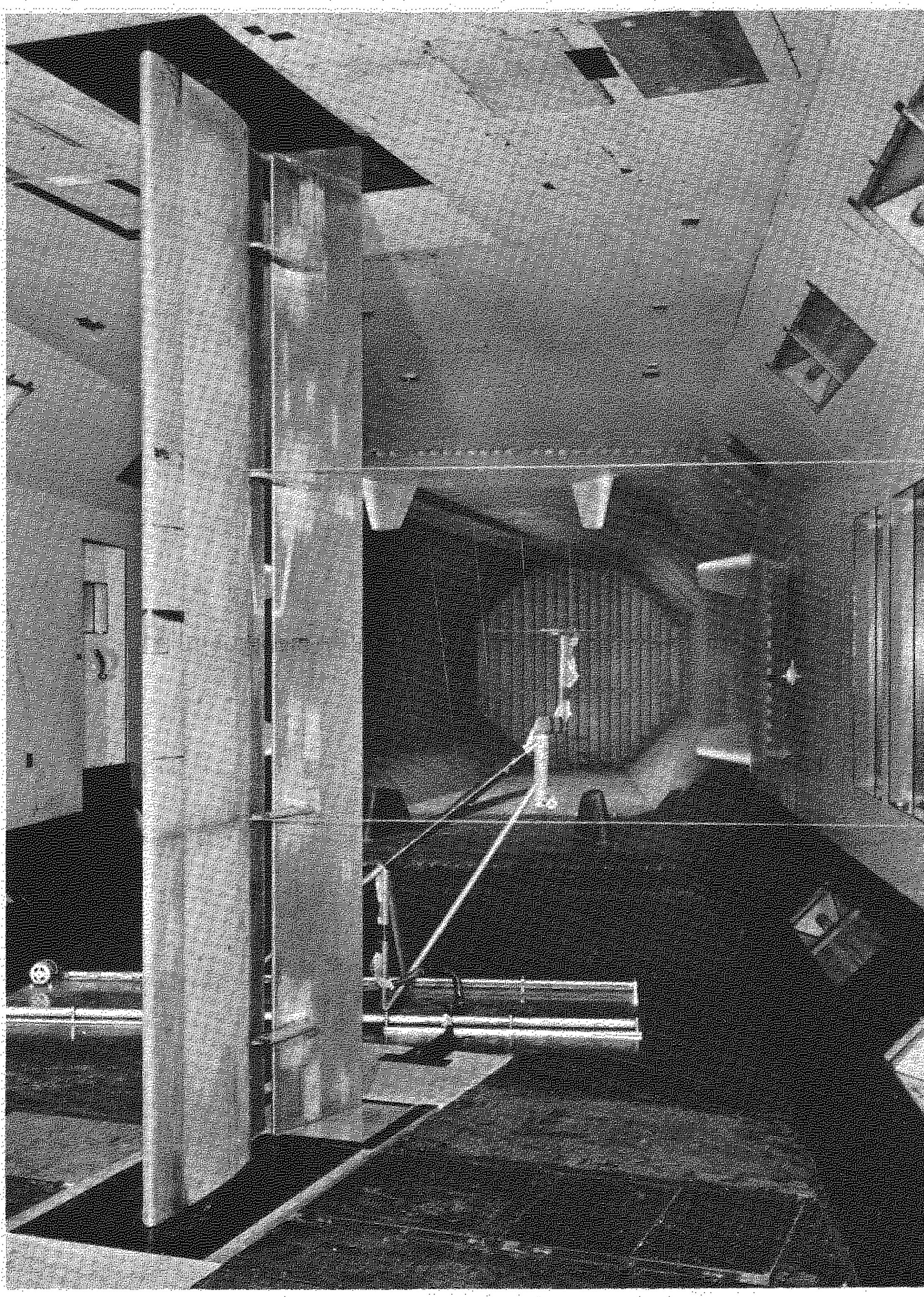

Fig.1. Wing section in wind tunnel

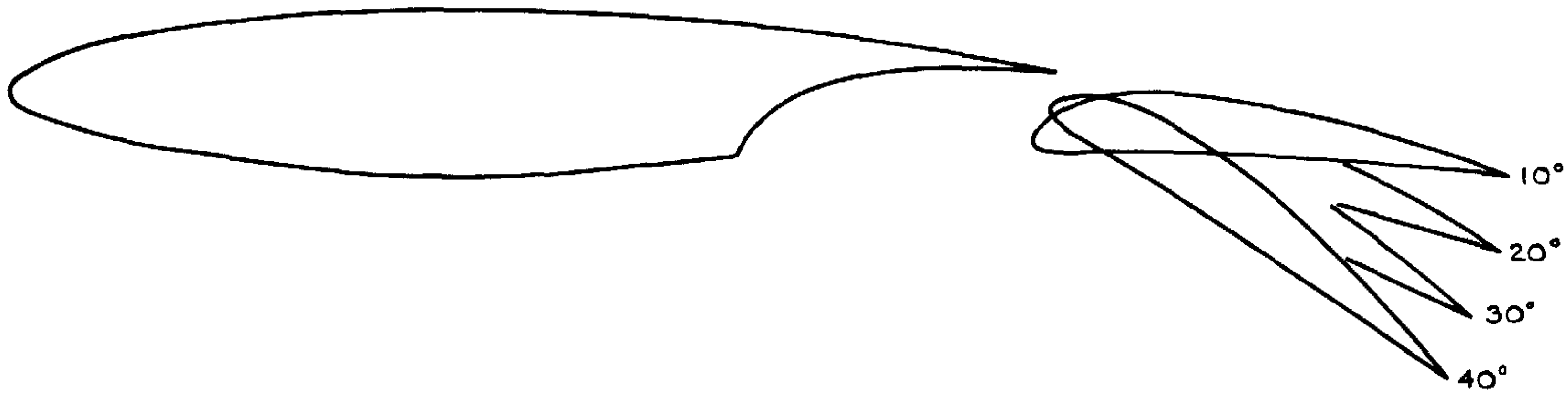

Fig. 2 Aerofoil section showing flap positions

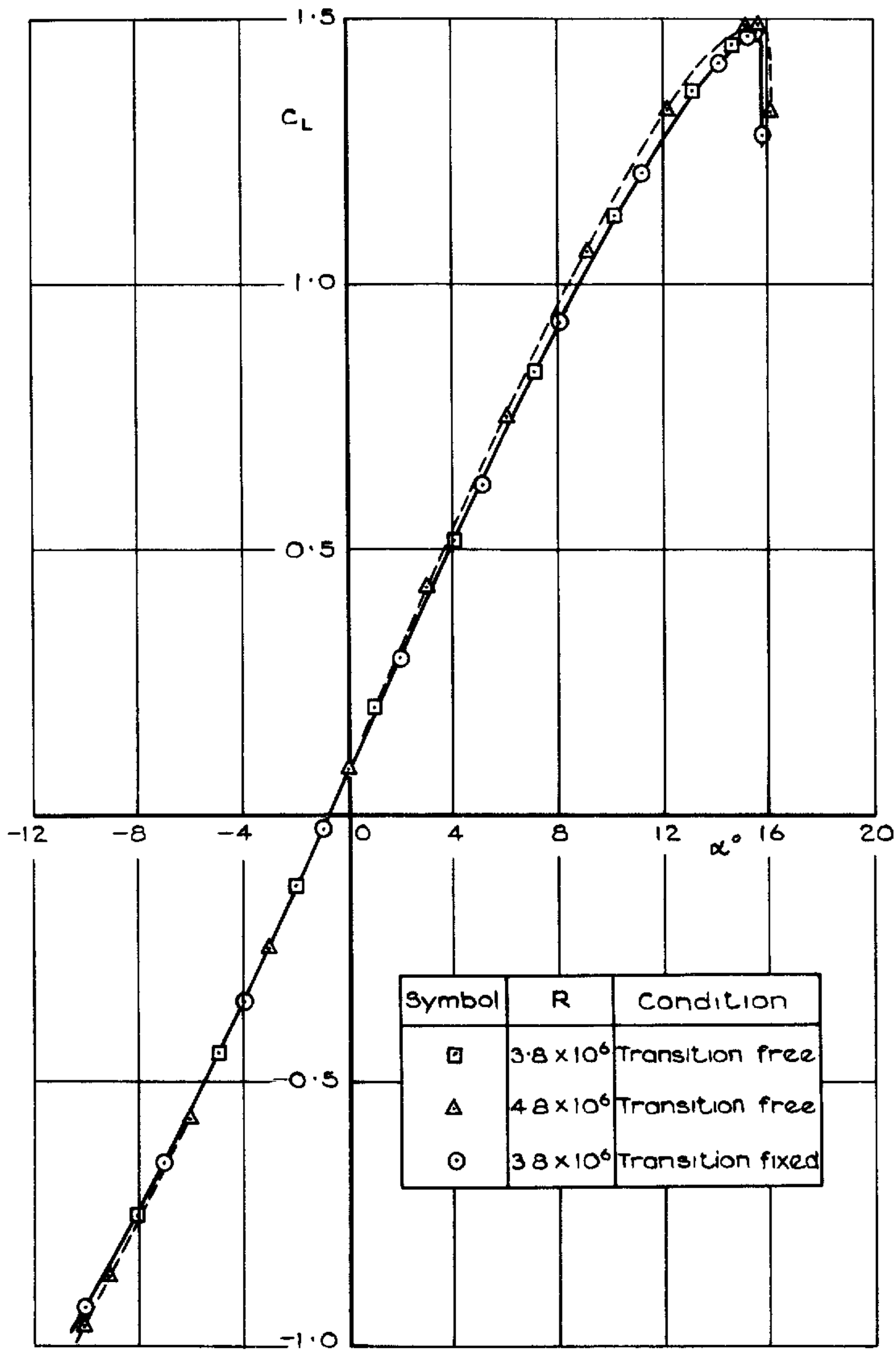

Fig.3 Lift curves for basic aerofoil section

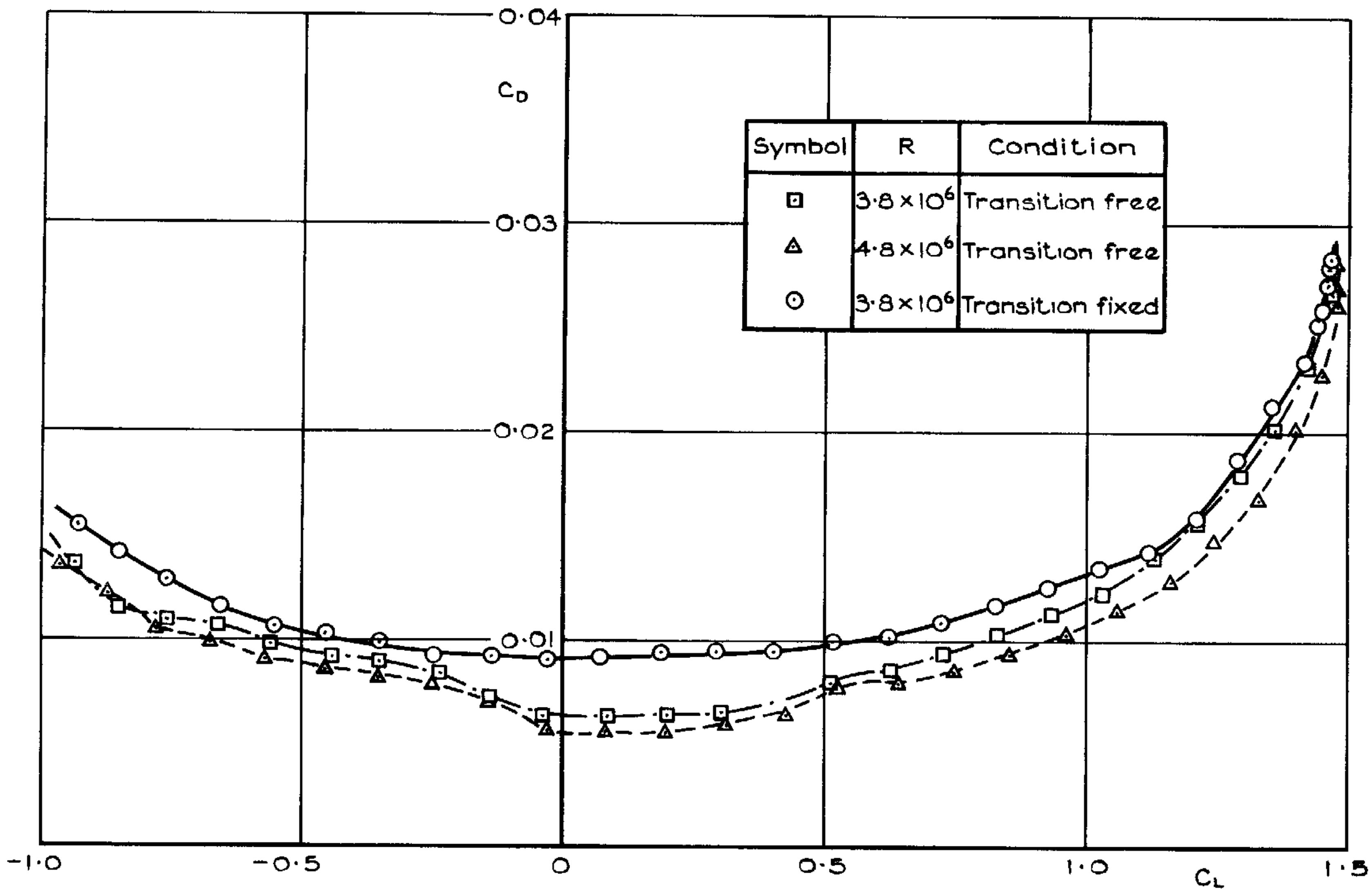

Fig. 4 Drag curves for basic wing section

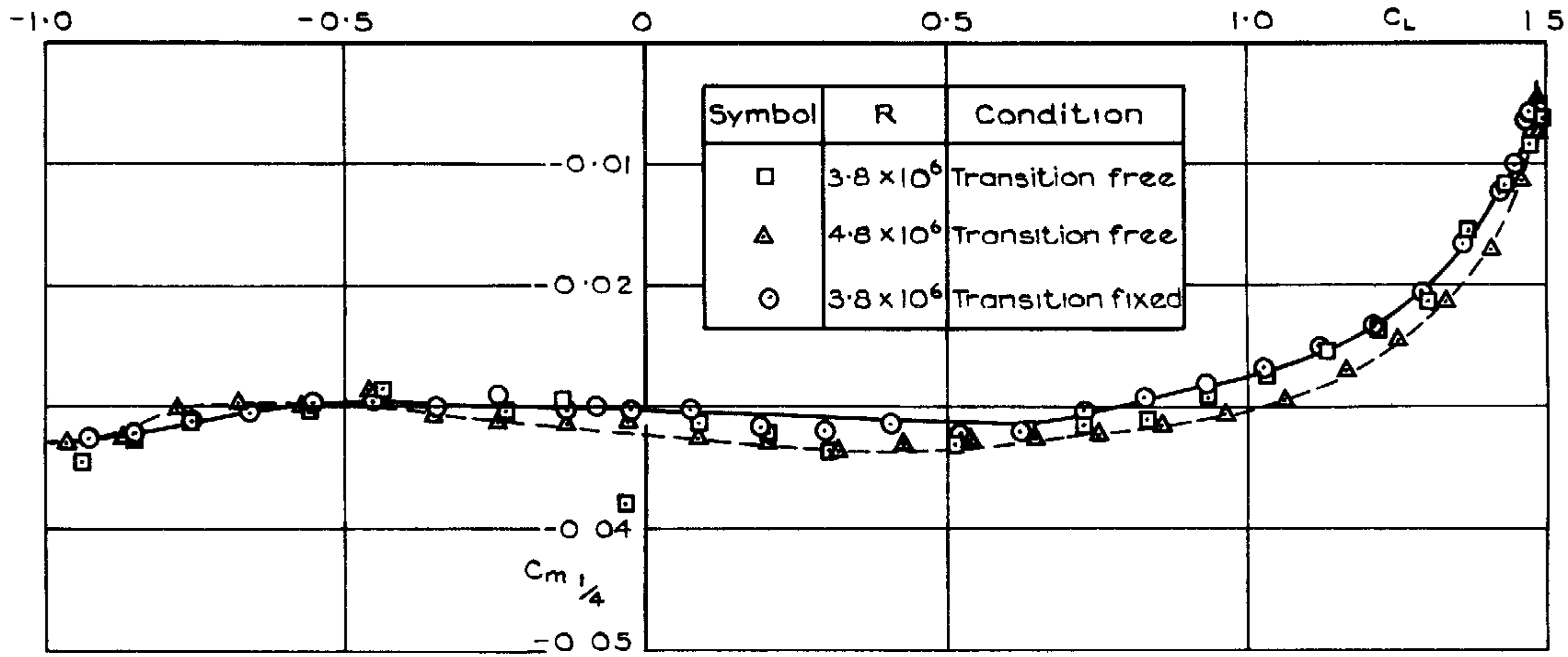

Fig.5 Pitching moment curves for basic section

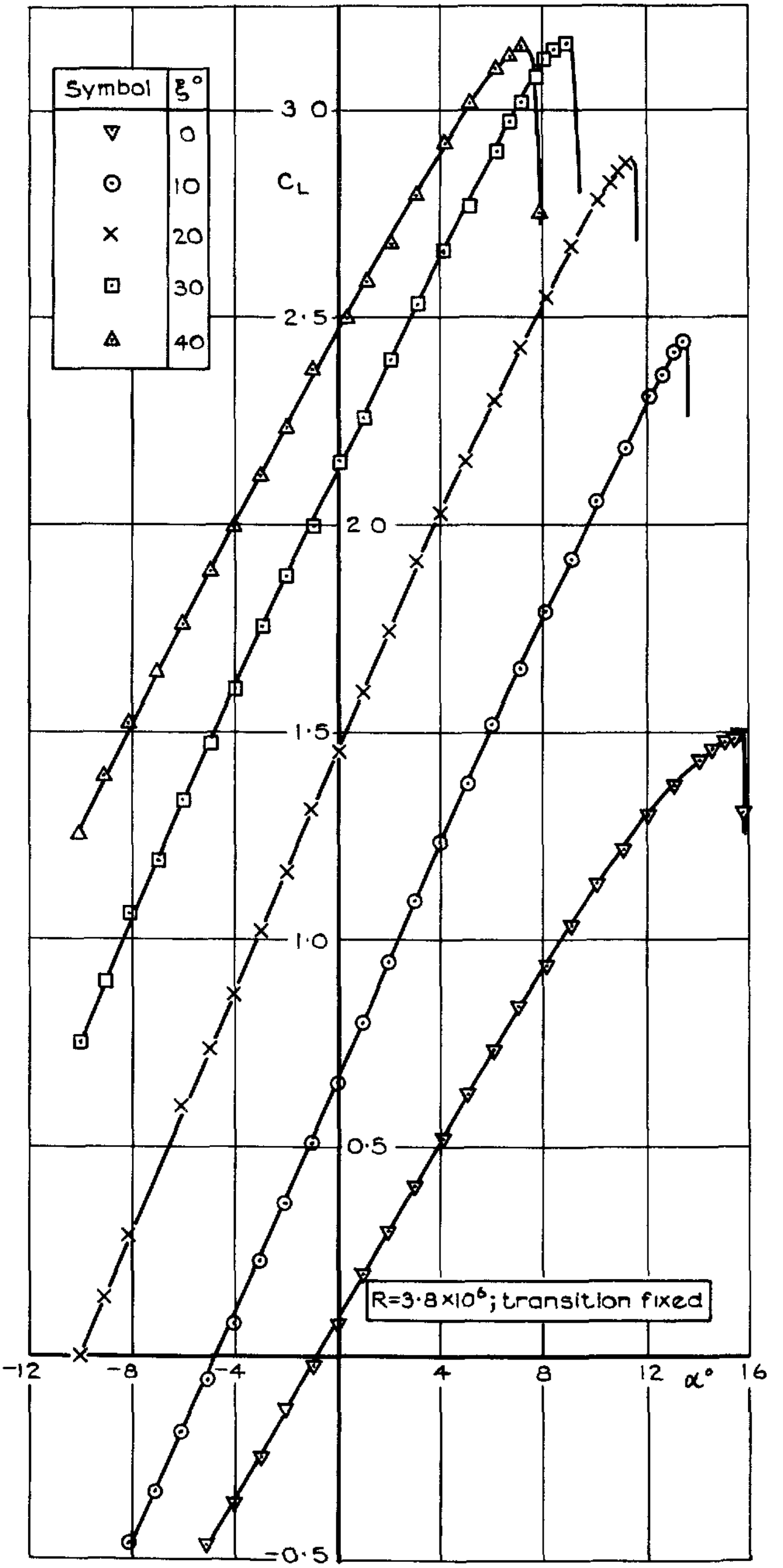

Fig 6 Effect of flap deflection on lift curves

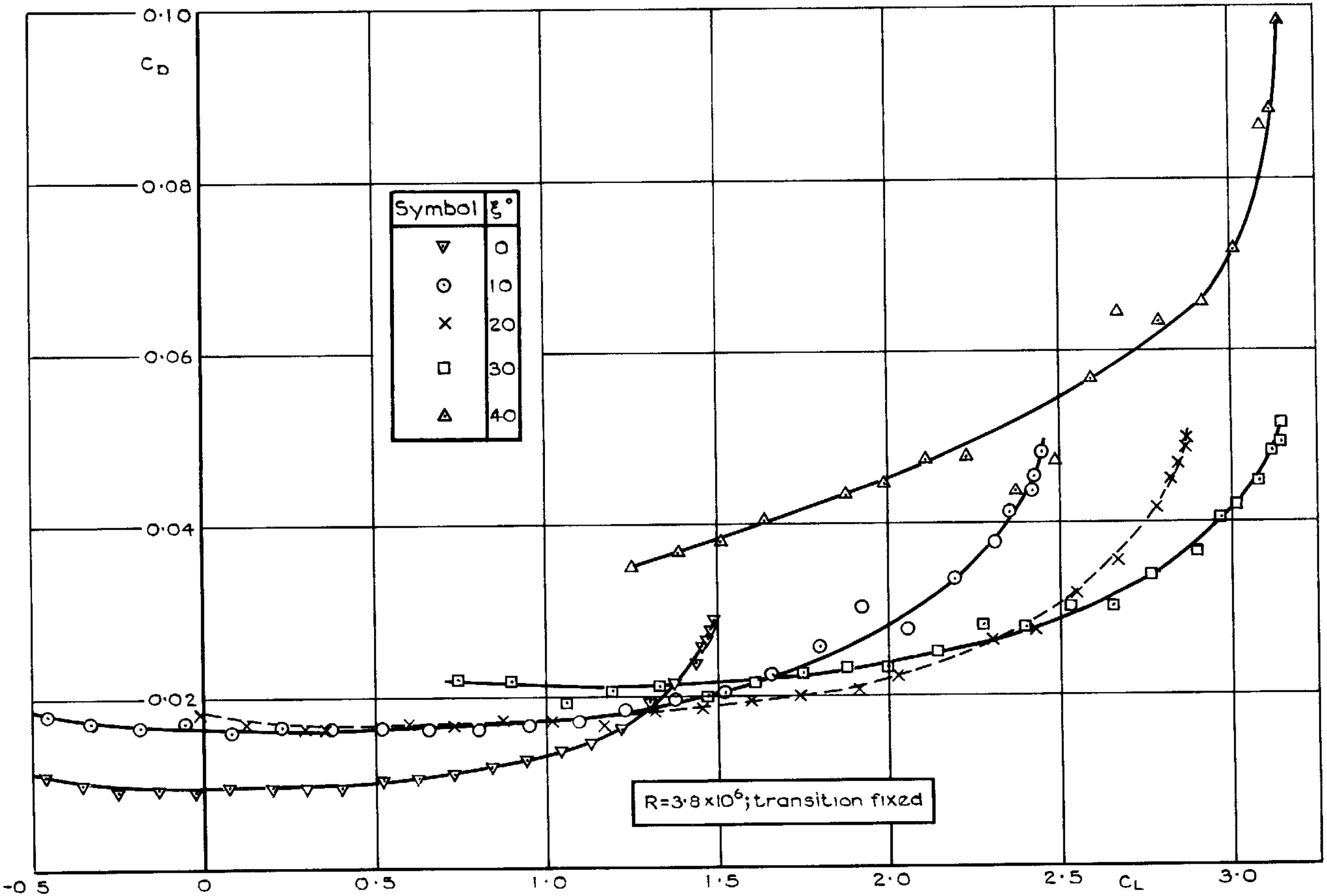

Fig. 7 Effect of flap deflection on drag curves

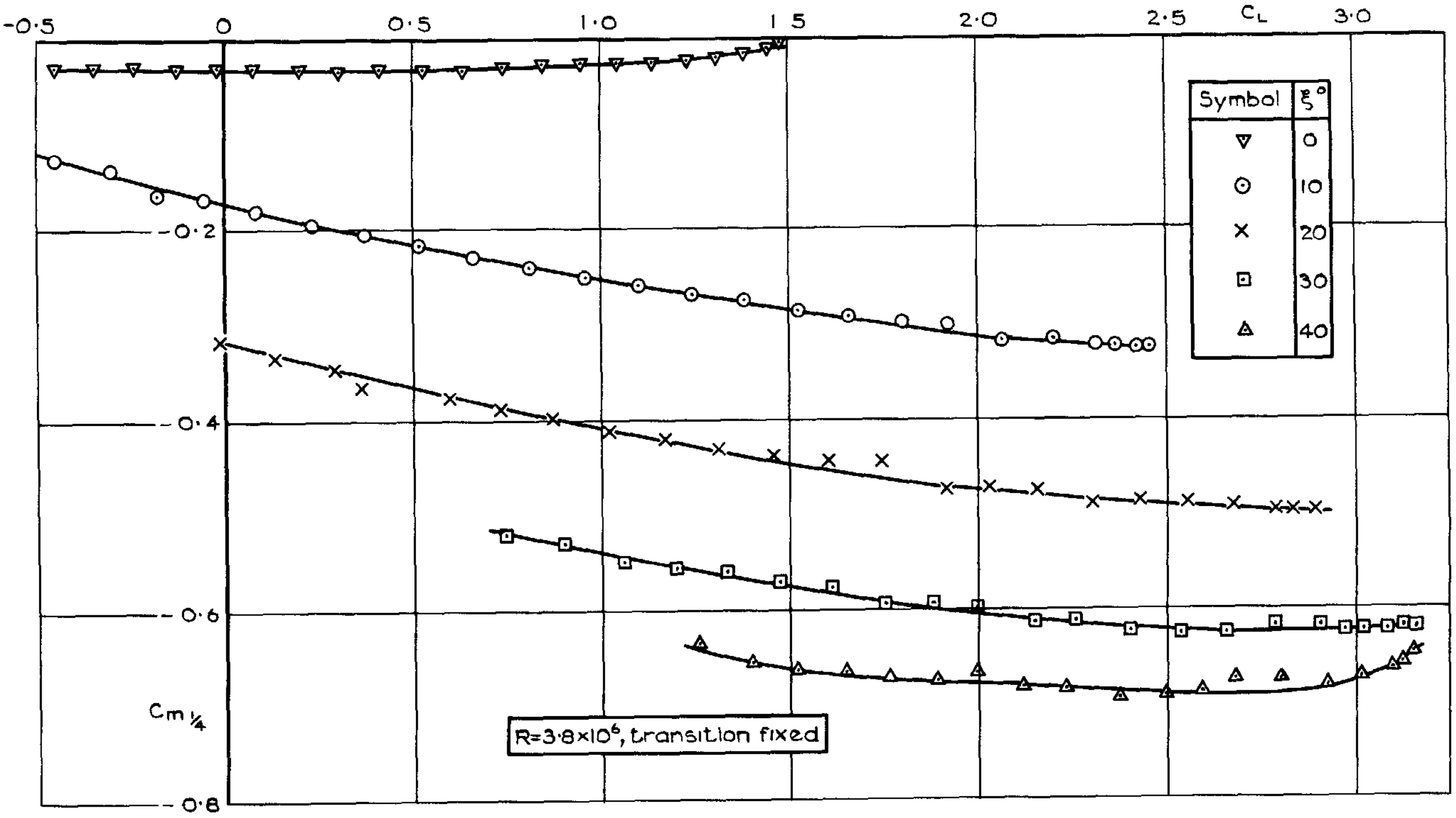

Fig.8 Effect of flap deflection on pitching moment curves

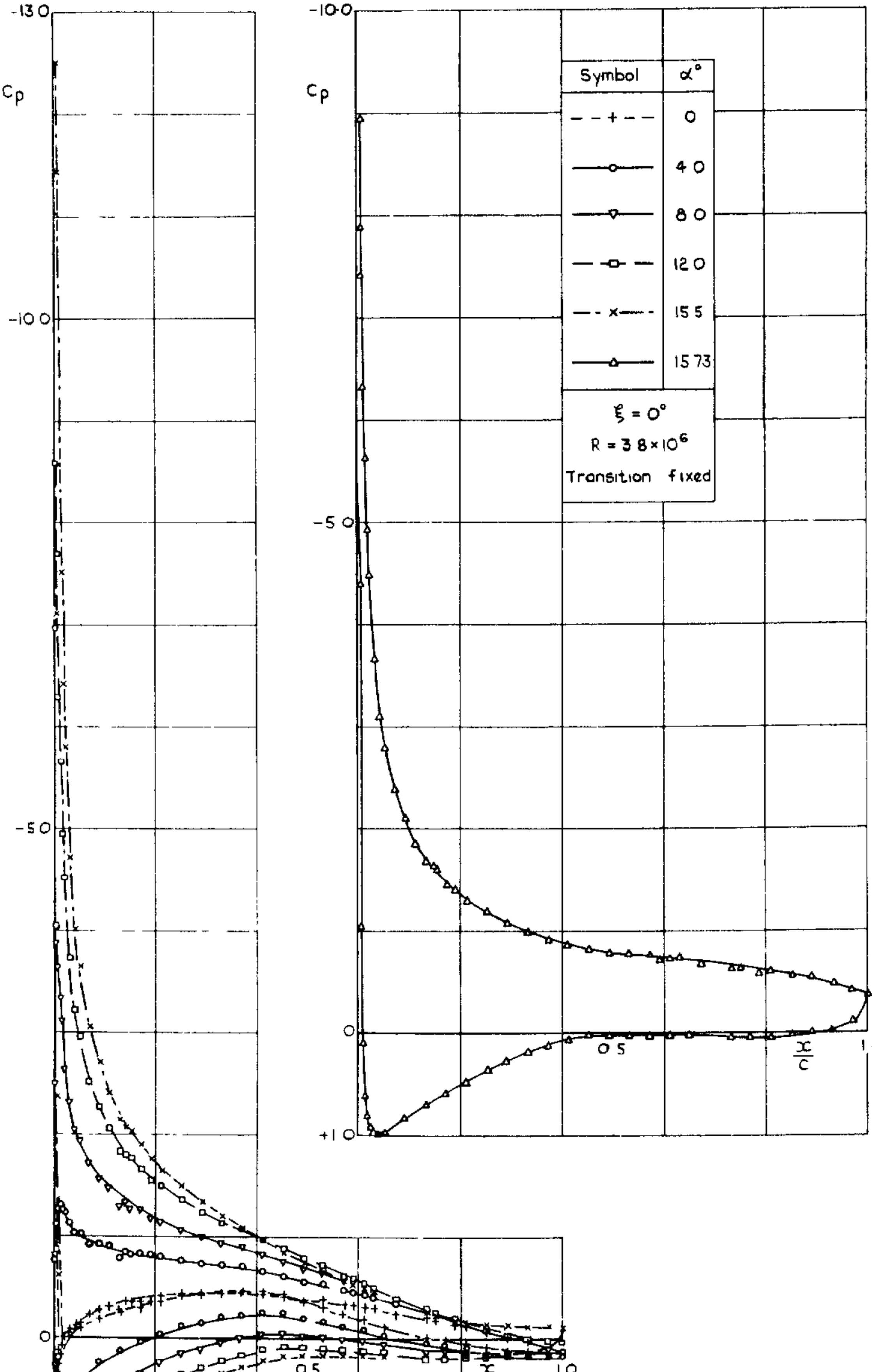

Fig. 9 Effect of angle of incidence on pressure distribution for basic wing. Stalled condition inset

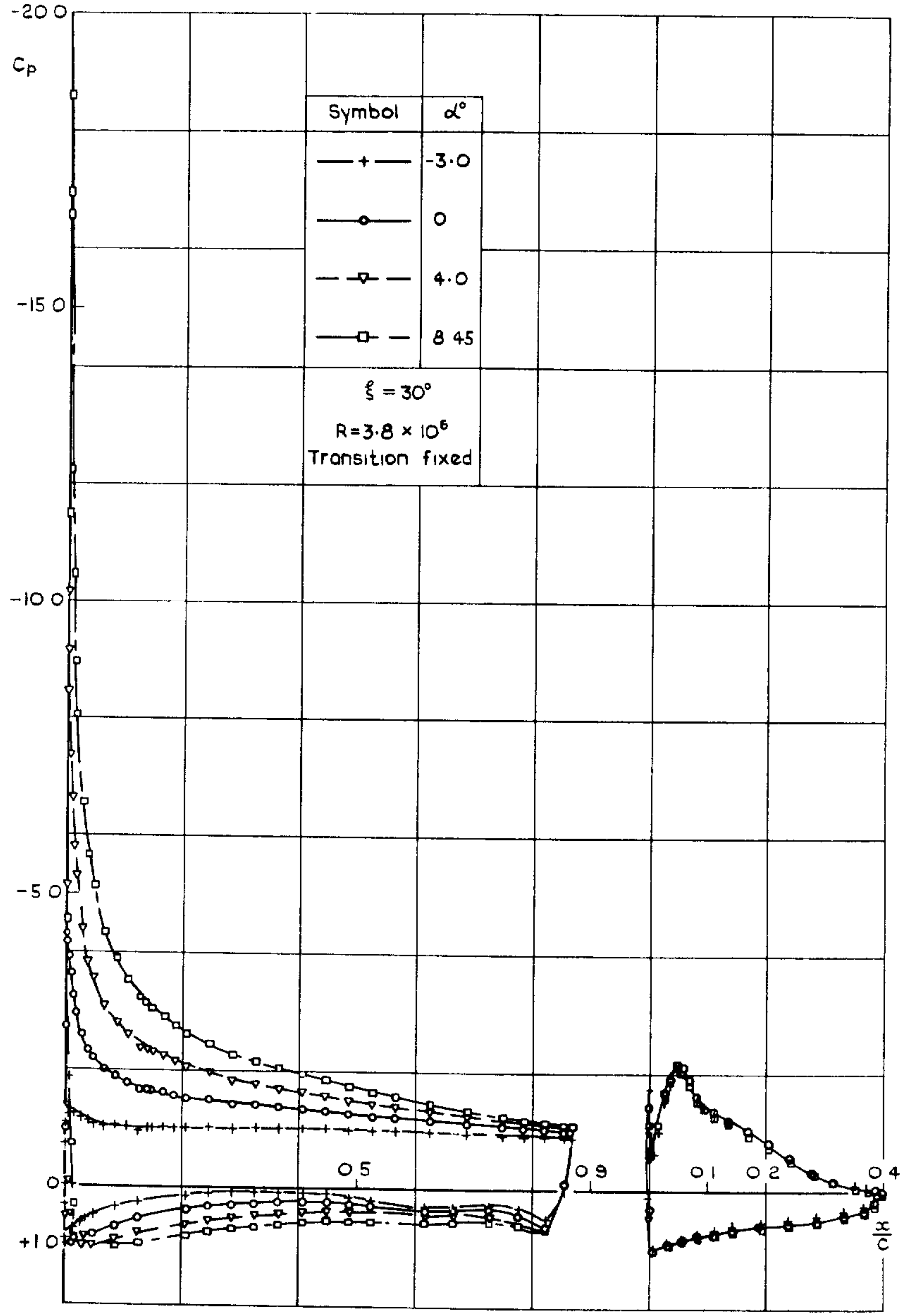

Fig.10 Effect of angle of incidence on pressure distribution

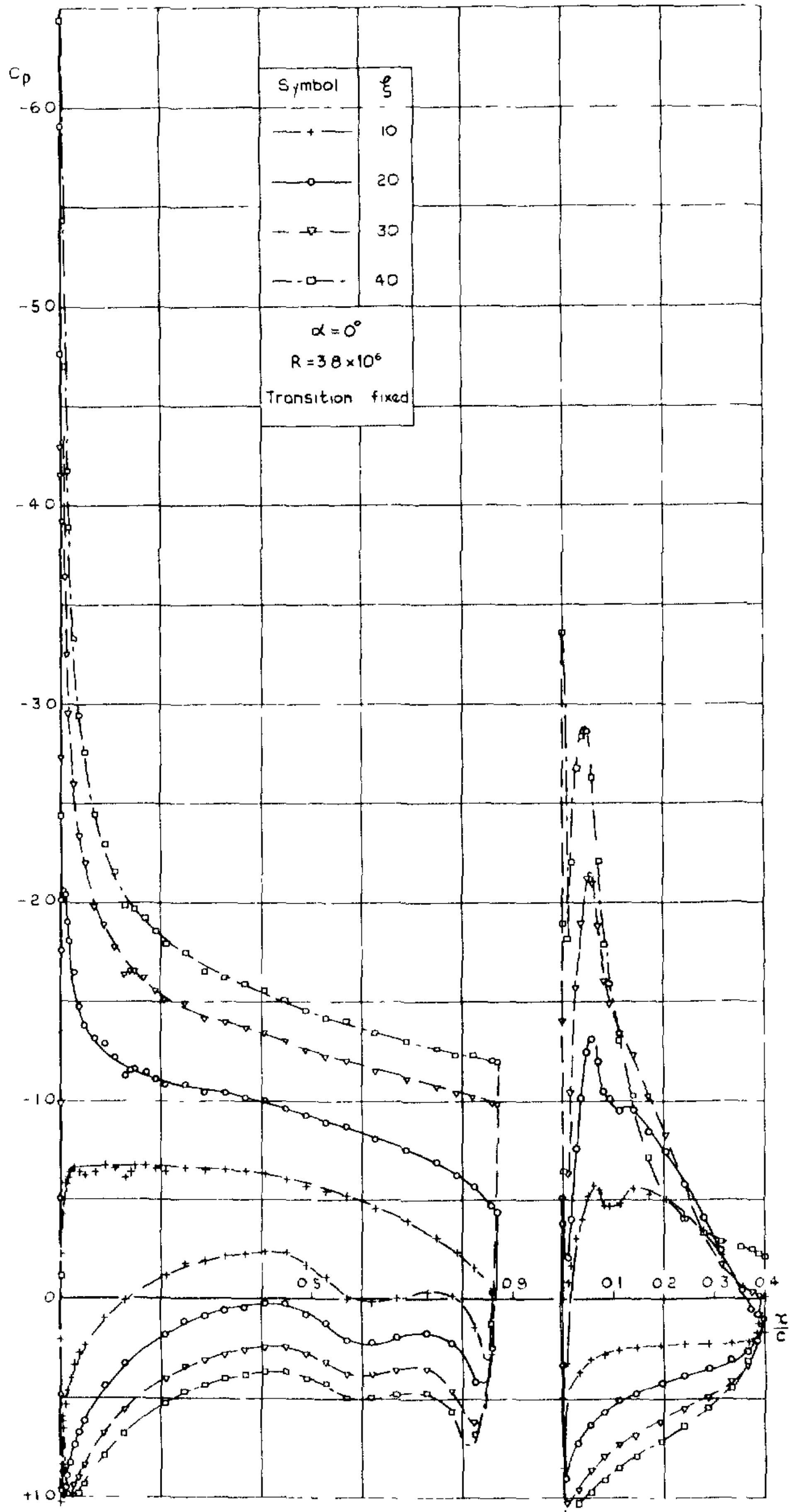

Fig.11 Effect of flap deflection on pressure distribution

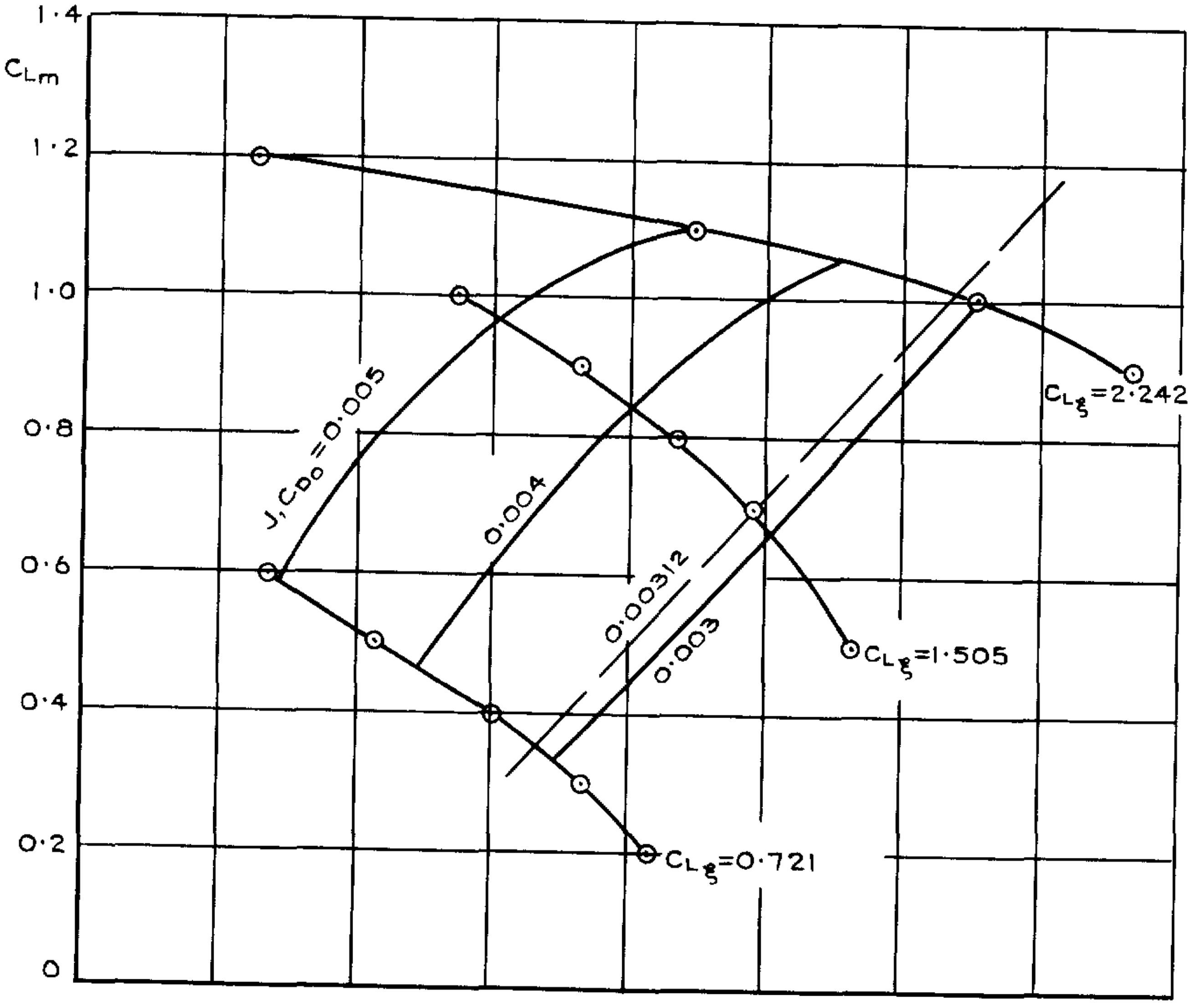

Fig. 12 Carpet plot to determine value of $J_1 C_{D_o}$

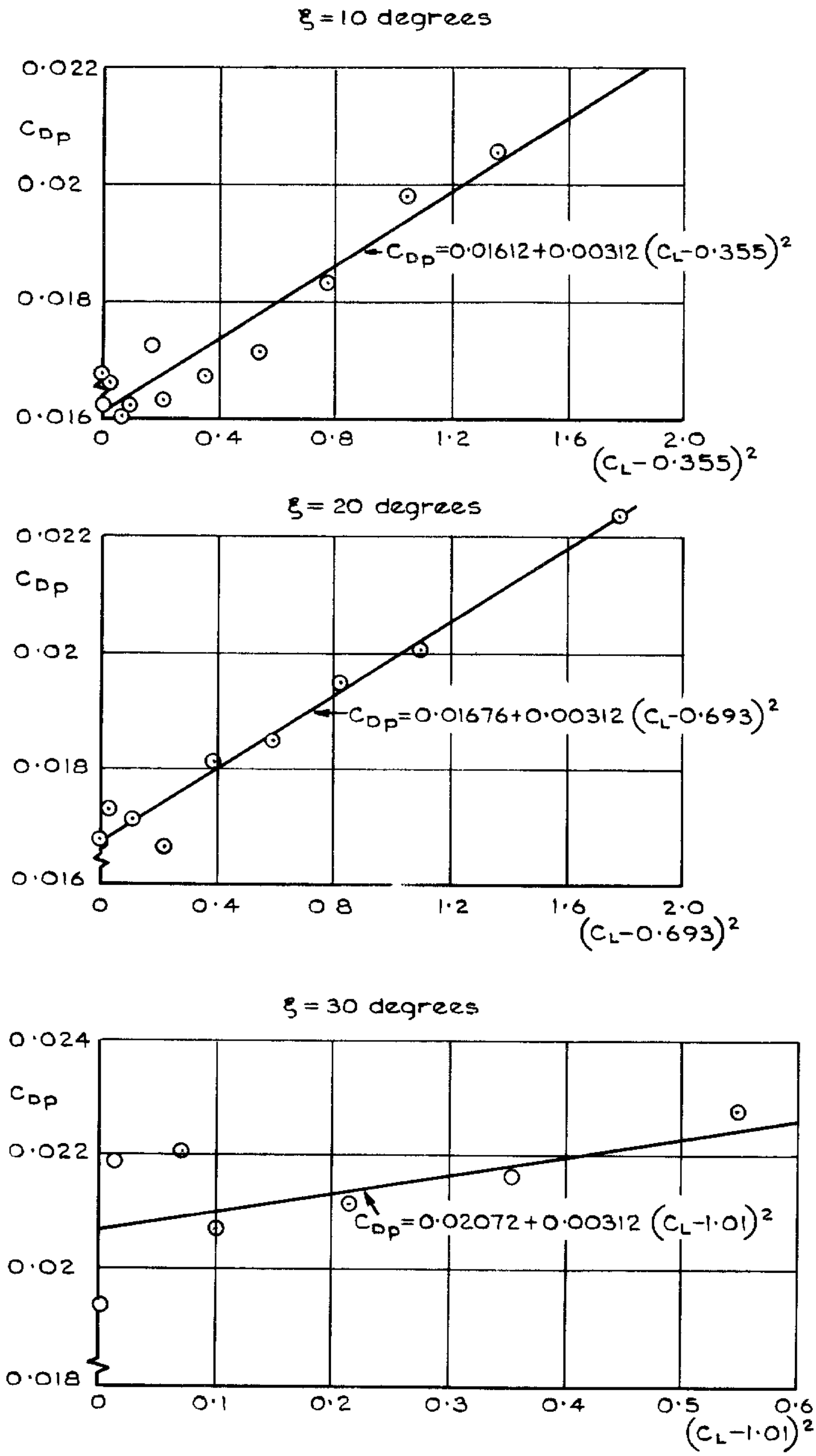

Fig. 13 Correlation of profile drag

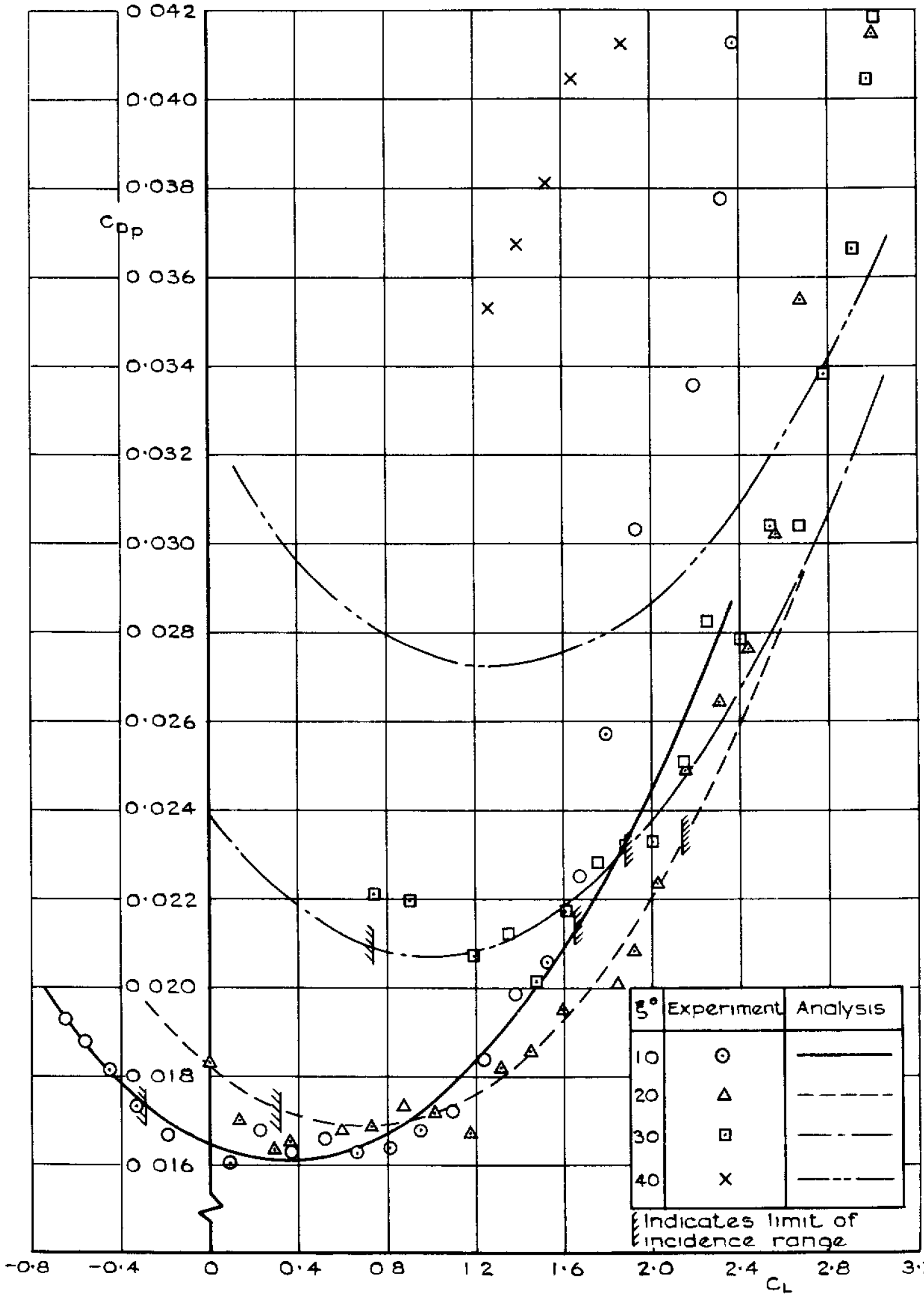

Fig. 14 Overall correlation of profile drag measurements

Printed in England for Her Majesty's Stationery Office by the Royal Aircraft Establishment Farnborough Dd 503427 K4 10/72

ARC CP No 1233
August 1971

533 6 013 122
533 692
533 694 22

I R M Moir
D N Foster
D R Holt

THE MEASUREMENT AND ANALYSIS OF THE PROFILE DRAG OF A WING WITH A SLOTTED FLAP

Measurements of lift, drag and pitching moments have been made on a wing section for a range of flap deflections, under conditions which were as close as possible to twodimensional flow. The corrected data are presented in this Report, together with the results of a semi-empirical analysis of sectional profile drag. It is shown that a consistent analysis can be made of the results over a range of flap angles and incidence, limited by a requirement for acceptable wing and flap boundary-layer conditions, precluding significant flow separations. Under these conditions, it appears that such an approach could serve as a general basis for correlating and interpreting experimental data on high-lift mechanical flap arrangements

These abstract cards are inserted in Technical Reports for the convenience of Librarians and others who need to maintain an Information Index

Detached cards are subject to the same Security Regulations as the parent document, and a record of their location should be made on the inside of the back cover of the parent document

— Cut here —

ARC CP No 1233
August 1971

533.6 013 122
533.692
533.694.22

I R M Moir
D N Foster
D R Holt

THE MEASUREMENT AND ANALYSIS OF THE PROFILE DRAG OF A WING WITH A SLOTTED FLAP

Measurements of lift, drag and pitching moments have been made on a wing section for a range of flap deflections, under conditions which were as close as possible to twodimensional flow. The corrected data are presented in this Report, together with the results of a semi-empirical analysis of sectional profile drag. It is shown that a consistent analysis can be made of the results over a range of flap angles and incidence, limited by a requirement for acceptable wing and flap boundary-layer conditions, precluding significant flow separations. Under these conditions, it appears that such an approach could serve as a general basis for correlating and interpreting experimental data on high-lift mechanical flap arrangements.

ARC CP No 1233
August 1971

533 6 013 122
533 692
533 694 22

I R M Moir
D.N Foster
D R Holt

THE MEASUREMENT AND ANALYSIS OF THE PROFILE DRAG OF A WING WITH A SLOTTED FLAP

Measurements of lift, drag and pitching moments have been made on a wing section for a range of flap deflections, under conditions which were as close as possible to twodimensional flow. The corrected data are presented in this Report, together with the results of a semi-empirical analysis of sectional profile drag. It is shown that a consistent analysis can be made of the results over a range of flap angles and incidence, limited by a requirement for acceptable wing and flap boundary-layer conditions, precluding significant flow separations. Under these conditions, it appears that such an approach could serve as a general basis for correlating and interpreting experimental data on high-lift mechanical flap arrangements.

— Cut here —

DETACHABLE ABSTRACT CARDS

DETACHABLE ABSTRACT CARDS

C.P. No. 1233

Published by
HER MAJESTY'S STATIONERY OFFICE

To be purchased from
49 High Holborn, London WC1 V 6HB
13a Castle Street, Edinburgh EH2 3AR
109 St Mary Street, Cardiff CF1 1JW
Brazennose Street, Manchester M60 8AS
50 Fairfax Street, Bristol BS1 3DE
258 Broad Street, Birmingham B1 2HE
80 Chichester Street, Belfast BT1 4JY
or through booksellers

C.P. No. 1233

SBN 11 470791 X